

First phase nickel silicide nucleation and interface structure at Si(100) surfaces

Yu-Jeng Chang and J. L. Erskine

Department of Physics, University of Texas, Austin, Texas 78712

(Received 29 September 1982; accepted 29 November 1982)

Photoemission and work function measurements are used to investigate the formation and structure of Ni-Si(100) interfaces at 300 K. For Ni coverages $\theta \leq 0.5 \text{ \AA}$ ($4.6 \times 10^{14}/\text{cm}^2$) a chemisorbed phase of Ni surface atoms forms. This chemisorbed phase persists to coverages $\theta \approx 2 \text{ \AA}$; but also in this coverage range, a diffusion layer forms in the Si lattice. At $\theta \approx 1.5 \text{ \AA}$ the surface composition closely resembles NiSi. Addition of more Ni atoms ($\theta > 1.5 \text{ \AA}$) initiates nucleation of Ni_2Si . The growth of this phase continues up to $\theta \approx 1.5 \text{ \AA}$ where silicide formation stops. Additional Ni atoms deposit as a pure Ni overlayer. These results yield a model for Ni-Si interfaces formed at room temperature which consists of a shallow diffusion layer of Ni atoms in the Si lattice, a very thin (1.5- \AA thick) interface having NiSi chemical characteristics, a Ni_2Si phase (15- \AA thick) of relatively uniform stoichiometry followed by a Ni layer.

PACS numbers: 68.55. + b, 68.48. + f, 73.30. + y, 79.60.Gs

I. INTRODUCTION

Current and anticipated applications of transition metal silicides in devices¹ and the failure of simple models to explain Schottky barrier heights in transition metal-silicon interfaces² has stimulated considerable efforts to characterize interface structure, growth kinetics, selective growth mechanisms, and electronic properties associated with transition metal silicides, and silicide based thin film structures and interfaces. Nickel silicides have received particular attention for several reasons. They form at relatively low temperatures, exhibit selective growth, and are easy to produce.³ In addition, several phases having different stoichiometries can be formed,⁴ and one particular phase (NiSi_2) forms a high quality epitaxial layer on Si(111) and Si(100) surfaces.

The Schottky barrier height of a metal semiconductor contact is determined by properties of the interfacial layer. In general, ionic large band gap materials can be described by the simple Schottky model,⁵ but highly polarizable covalent materials cannot.^{2,5} More complex models based on surface states,⁶ interface dipoles,⁷ and interface chemistry⁸⁻¹⁰ have been proposed, but these models all rely on a detailed description of the interface structure or electronic properties. Important progress toward a more detailed understanding of transition metal interfaces (Ni-Si interfaces in particular) has been made in recent years using x-ray diffraction,¹¹⁻¹³ ^4He ion channeling,¹²⁻¹⁸ x-ray¹⁹⁻²³ and ultraviolet²⁴⁻²⁹ photoelectron emission spectroscopy (XPS and UPS), and electron diffraction including transmission electron diffraction³⁰ (TEM), low energy electron diffraction,^{31,32} and high energy electron diffraction.

Ion backscattering and channeling have established the dominant species involved in mass transport during silicide growth^{17,18} and have shown that epitaxial layers of several silicides including NiSi_2 can be formed.¹⁴ The same techniques have also been used to probe the areal density of displaced atoms diffused near the surface¹⁵ and at the interface between epitaxial NiSi_2 and Si crystals.¹⁴ XPS and UPS have established the reaction kinetics associated with planar silicide growth and the process dependence of interfacial struc-

ture in silicon-transition metal systems.¹⁹⁻²⁶ UPS²⁷⁻²⁹ in conjunction with electronic structure calculations^{29,32,33} have established a number of important features associated with bulk nickel silicides including the *d*-state binding energy dependence on Ni-Ni interactions in stoichiometric compounds and the ground state electronic structure.

In addition, several models have been proposed to explain the low temperature growth and phase formation of certain metal silicides. Interstitial diffusion of metal atoms into Si lattice voids at the growth interface has been postulated to account for the observed silicide growth at temperatures considerably below compound melting points.³ Recent MeV ^4He ion channeling¹⁵ and photoelectron emission³⁴ studies have obtained evidence for this model. A rule which predicts the first phase formed at an interfacial layer has also been proposed. This rule predicts the existence of an amorphous interfacial layer with composition near the binary system eutectic.³⁵ These growth mechanisms and phase nucleation rules have important bearing on the formation and structure of metal semiconductor interfaces.

In the present study we have used ultraviolet photoemission and work function measurements to investigate the room temperature interface formation of Ni-Si interfaces at Si(100). Our work supports recent ion channeling results¹⁵ and XPS studies²⁰ which indicate strong chemical interactions between the first few monolayers of Ni deposited on Si at room temperature. We find evidence of interstitial diffusion at the Si interface³ in interfaces formed at room temperature. Our results show that a thin layer of Ni_2Si nucleates at room temperature in agreement with the "first phase rule"³⁵ and also provides a fairly detailed description of the structure and chemical characteristics of Ni-Si interfaces produced by metal deposition at 300 K.

II. EXPERIMENTAL TECHNIQUES

Our experiments were carried out using a spectrometer, described previously,³⁶ which combines low energy electron diffraction (LEED), Auger electron spectroscopy, and photoemission capabilities. Two features of our spectrometer

were important in conducting the work reported here. One feature is a high intensity resonance lamp based on a design reported by Shevchik.³⁷ High counting rates are achieved at better than 100-meV resolution. This permits rapid signal averaging to statistical noise levels below 1%. A second important feature used in the present work is the capability to transmit data to a computer for curve fitting analysis and spectra decomposition. Our work function data was obtained by measuring the width of the photoelectron energy distribution curves produced by the He I radiation ($h\nu = 21.22$ eV).

A vacuum evaporation source and quartz crystal microbalance permitted *in situ* preparation of Ni-Si interface structures. The microbalance was calibrated by compiling a table of frequency shifts versus layer thickness measured using optical interferometry. Auger spectroscopy provided a monitor of surface composition during evaporation as well as a consistency check of the thickness. Typical spectrometer base pressures were 1×10^{-10} Torr, 3×10^{-9} Torr during He resonance lamp operation, and 9×10^{-9} Torr during Ni deposition.

The 3/8-in.-diam \times 0.020-in.-thick Si targets were cut from B-doped 50 Ω cm-oriented (100) wafers provided by Monsanto. The targets were clamped to a ceramic ring by two 0.030-in.-diam W wires. Targets were degreased using standard techniques and cleaned *in situ* by repeated argon ion sputtering (500 eV, $10 \mu\text{A}/\text{cm}^2$) and annealing (800 $^\circ\text{C}$). Sample temperatures were measured by a W-5% Re vs W-26% Re thermocouple in mechanical contact with the sample. This procedure produced clean Si surfaces which yielded sharp (2×1) LEED patterns and distinct surface state peaks in photoemission spectra. No indication of surface impurities was detected from Auger analysis.

III. EXPERIMENTAL RESULTS

Figure 1 shows photoemission energy distribution curves (EDCs) for low coverage Ni layers ranging from 0 to 5 \AA on clean Si(100) 2×1 . The Fermi energy was determined from metallic bulk silicides and Ni overlayers after the low coverage work was completed. Corresponding work function data are shown in Fig. 2. The photoemission and work function results show several distinct phases occur as Ni atoms are deposited onto Si(100) at 300 K. Detailed analysis requires decomposition of EDC's, discussed later, however, some of the changes are apparent directly from the data.

The first phase occurs for Ni coverages ranging from 0 to 0.5 \AA ($4.6 \times 10^{14}/\text{cm}^2$). This coverage range is characterized by chemisorbed Ni atoms on the Si(100) surface. Quenching of the surface states and abrupt disorder observed in LEED are manifestations of the strong chemical bonding effects. It is clear from Fig. 1 that a 0.25- \AA layer of Ni quenches the two surface states observed at binding energies of 1.0 and 0.8 eV in the clean Si(100) 2×1 spectra. The work function data also shows an abrupt decrease in the work function between clean Si(100) 2×1 and 0.5- \AA Ni coverages. The sign of the work function change is consistent with charge transfer³² from Ni to Si atoms assuming the Ni atoms remain on the surface. This charge transfer represents additional evidence

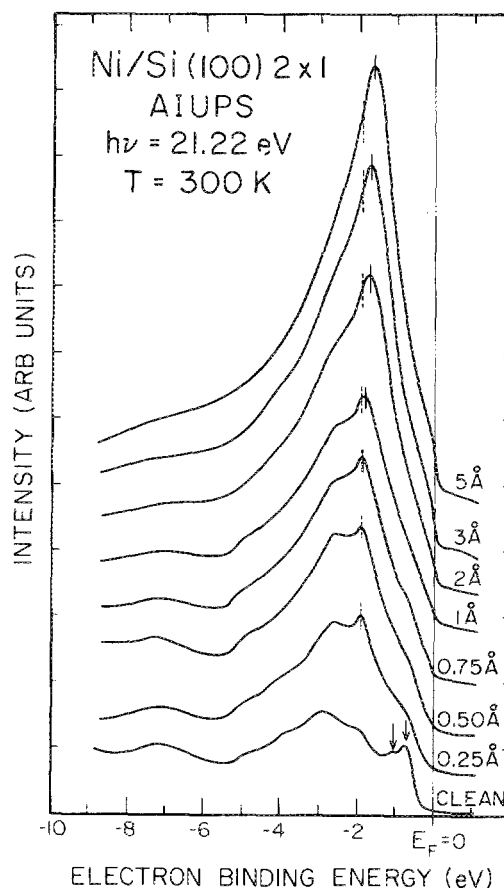


FIG. 1. Angle-integrated photoemission spectra ($h\nu = 21.22$ eV) of Ni layers ranging from 0.25 to 5 \AA deposited at 300 K on Si(100). Energy resolution \sim 100 meV, statistical error \sim 1%. Solid line through peak represents Ni *d*-state binding energy. Arrows indicate Si(100) 2×1 surface states.

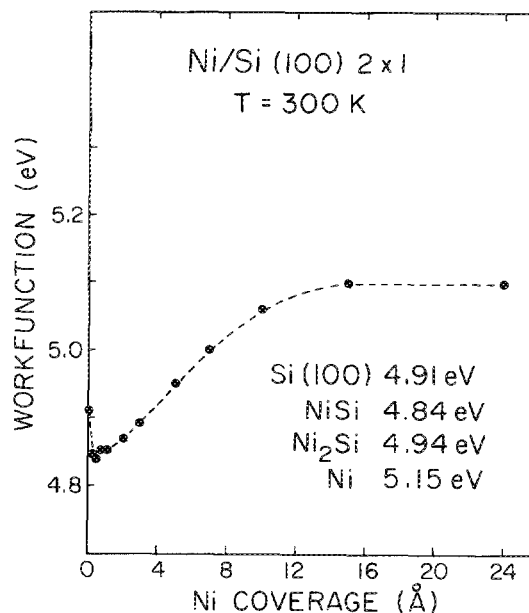


FIG. 2. Work function data for Ni layers ranging from 0.25 to 25 \AA deposited at 300 K on Si(100). Inset table shows work function results for clean Si(100) 2×1 , evaporated Ni, and two bulk silicide compounds NiSi and Ni₂Si.

of a strong chemical reaction between Ni and Si at room temperature.

Additional changes begin to occur at approximately $0.5\text{-}\text{\AA}$ Ni coverages indicating a distinct new chemisorption regime. The work function begins to increase, and the d -state binding energy (designated by a solid line through the appropriate peaks in Fig. 1) begins to shift toward the Fermi level. A $0.5\text{-}\text{\AA}$ thickness corresponds to substantially less than one monolayer of Ni, and the changes must be due to some interaction mechanism between Ni atoms. The increase in work function could be caused by clustering of Ni atoms on the surface (which would tend to form metalliclike islands with a local work function more like metallic Ni), or by formation of the metal rich silicide Ni_2Si . Also, it could be caused by diffusion of Ni atoms into the Si lattice. Experimental evidence clearly favors diffusion, as will be discussed in more detail later.

At Ni atom coverages of approximately $0.75\text{ }\text{\AA}$, the d -state binding energy is about 1.9 eV , which is very close to the value we have obtained for thick ($200\text{ }\text{\AA}$) films of NiSi stoichiometry produced by reacting evaporated Ni with $\text{Si}(100)$ at 400°C . The work function at $1\text{-}\text{\AA}$ coverage is $\sim 4.85\text{ eV}$, which is very close to the value we have obtained for the bulk NiSi films.³⁴ This phase is not the stable composition at room temperature because as more Ni atoms are added, the reaction continues. At a coverage of $5\text{ }\text{\AA}$, the d -state binding energy has shifted to 1.4 eV , a value very close to results obtained for bulk samples²⁹ and thick films³⁴ of Ni_2Si produced by reacting Ni films with Si at 250°C .¹² The work function at $5\text{-}\text{\AA}$ coverage is also very close to the value we have obtained for the bulk samples²⁹ and thick films³⁴ of Ni_2Si stoichiometry. We therefore see that at room temperature, the chemical reaction between Ni and Si tends to nucleate Ni_2Si provided a sufficient number of Ni atoms are present. This result is what is expected based on the first phase formation rule suggested by Walser and Bené.³⁵

Compound nucleation of Ni_2Si continues to occur at room temperature until approximately $10\text{ }\text{\AA}$ of Ni have been deposited. Work function changes show that the stoichiometry at the surface is not constant, and that a graded nickel rich interface is formed as seen in XPS studies.²⁰ After $10\text{ }\text{\AA}$ coverage, room temperature mass transport through the silicide necessary to support growth of the silicide interface stops, presumably due to low room temperature diffusion constants for Ni and silicon in Ni_2Si . Additional layers of Ni atoms do not react, and begin to form a Ni film. Planar phase growth can be activated by heating the film to above 250°C .

Additional insight into the room temperature interface formation can be gained by a more detailed analysis of the EDC's. Figure 3 illustrates decomposition of the spectra for two coverages: 0.25- and $0.50\text{-}\text{\AA}$ Ni. In Fig. 3(b), the difference spectra (dotted curve), obtained by subtracting the clean $\text{Si}(100) 2\times 1$ spectra from the $0.25\text{-}\text{\AA}$ Ni spectra, is compared with the spectra for bulk NiSi . Low coverage EDC's were normalized by using the bulk Si feature at $\sim 7\text{ eV}$ below E_F to adjust the scale before obtaining difference curves. The primary features corresponding to Ni d states occur at the same binding energy. Previous work has established that the d -state binding energy is related to the Ni-Ni interaction,^{29,34} therefore the binding energy characterizes

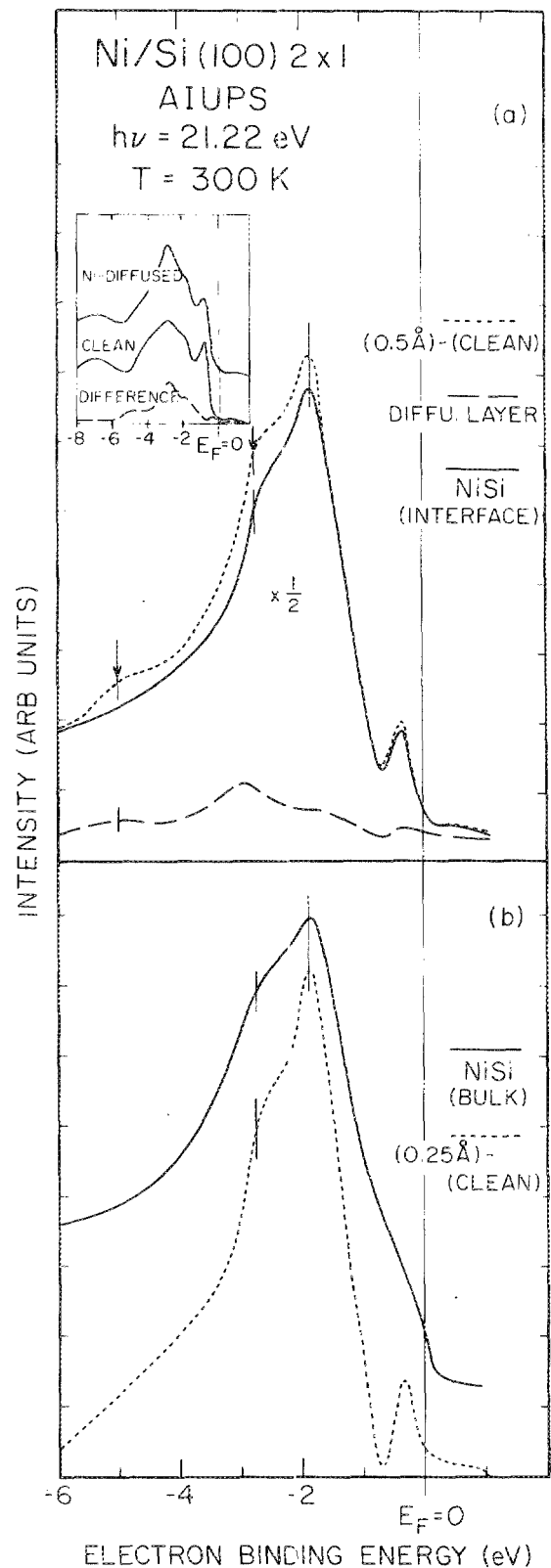


FIG. 3. Lower panel (a): Dotted curve, difference spectra obtained by subtracting clean Si spectra from $0.25\text{-}\text{\AA}$ Ni spectra of Fig. 1. Solid curve bulk NiSi spectra. Upper panel (b): Dotted curve, difference spectra obtained by subtracting clean Si spectra from $0.50\text{-}\text{\AA}$ Ni spectra of Fig. 1; inset diffusion layer data for $\text{Si}(100)$, see the text and Ref. 12, both dashed curves represent diffusion layer difference spectra (from inset); solid curve, difference spectra after subtraction of diffusion layer contribution. Arrows shows features due to diffusion layer.

the "surface" stoichiometry or chemical state. At low coverages, up to $\sim 1 \text{ \AA}$, the ratio resembles NiSi .

Figure 3(a) shows an analogous plot for a 0.5-\AA Ni average. The dotted curve again represents a difference curve obtained by subtracting the clean $\text{Si}(100) 2 \times 1$ spectra from the 0.5-\AA Ni coverage spectra. This curve shows evidence of diffusion layer formation in the Si lattice (as suggested by the work function results discussed in relation to Fig. 2). In order to support this claim, a difference curve corresponding to the diffusion layer in $\text{Si}(100) 2 \times 1$ is obtained in the inset of Fig. 3(a). In the inset, the two solid curves correspond to clean $\text{Si}(100) 2 \times 1$ with a diffusion layer of Ni atoms in Si lattice voids. This work is described in detail elsewhere.³⁴ The main points required for discussion here are: (1) the diffusion layer exists at a Ni concentration which corresponds to NiSi_2 stoichiometry based on the observed d -state binding energy (refer to lower curve of inset which shows difference curve) and (2) the diffusion layer does not destroy the surface states or the 2×1 LEED pattern. The diffusion layer difference curve is reproduced as the dashed lower curve of Fig. 3(b), and the solid line is obtained by subtracting the diffusion layer spectra from the 0.5-\AA -thick Ni difference curve. After subtraction of the diffusion layer spectra, the spectra for 0.5- and 0.25-\AA Ni coverages are nearly identical. The difference spectra provide evidence that a diffusion layer forms at room temperature at Ni atom coverages in the $0.25\text{--}0.50 \text{ \AA}$ Ni coverage range. This result is consistent with our work function data, and agrees with the conclusion reached based on $\text{MeV } ^4\text{He}$ channeling studies of "as-deposited" Ni layers.¹⁵

Figures 4(a)–4(c) continue a similar procedure for thicker films. Based on the results shown in Figs. 1 and 2, we postulate Ni_2Si begins to nucleate at $\sim 1 \text{ \AA}$. Therefore, difference spectra for films $\sim 1\text{-\AA}$ thick are assumed to contain contributions from the diffusion layer, the chemisorbed NiSi interface and the Ni_2Si phase which begins to nucleate. The decompositions shown in Figs. 4(b) and 4(c) represents a "best fit" obtained by trial and error synthesis based on these three contributions.

Figure 4(a) shows a difference curve obtained by subtracting the 3-\AA Ni coverage EDC from the 5-\AA Ni coverage EDC. This spectra is representative of the top 2 \AA of a 5-\AA film of Ni deposited on Si at room temperature. This difference spectra is compared with the spectra for bulk Ni_2Si films produced by annealing 200-\AA thick Ni layers on $\text{Si}(100) 2 \times 1$. The Ni d -state binding energies are the same for both spectra showing clearly the top 2 \AA of a 5-\AA film nucleates as Ni_2Si . The rather large difference in background is due to the fact that secondary electron contributions are subtracted out (to a large extent) in the difference curves.

IV. SUMMARY AND CONCLUSIONS

Application of this procedure to several Ni films deposited at room temperature and ranging in thickness from below 0.25 \AA to over 25 \AA has led us to the following conclusions regarding room temperature Ni–Si interfaces grown on $\text{Si}(100) 2 \times 1$: The first deposited Ni atoms form a chemisorbed phase of surface atoms. This phase persists from very low coverages up to about 1 \AA of deposited Ni. Beginning at

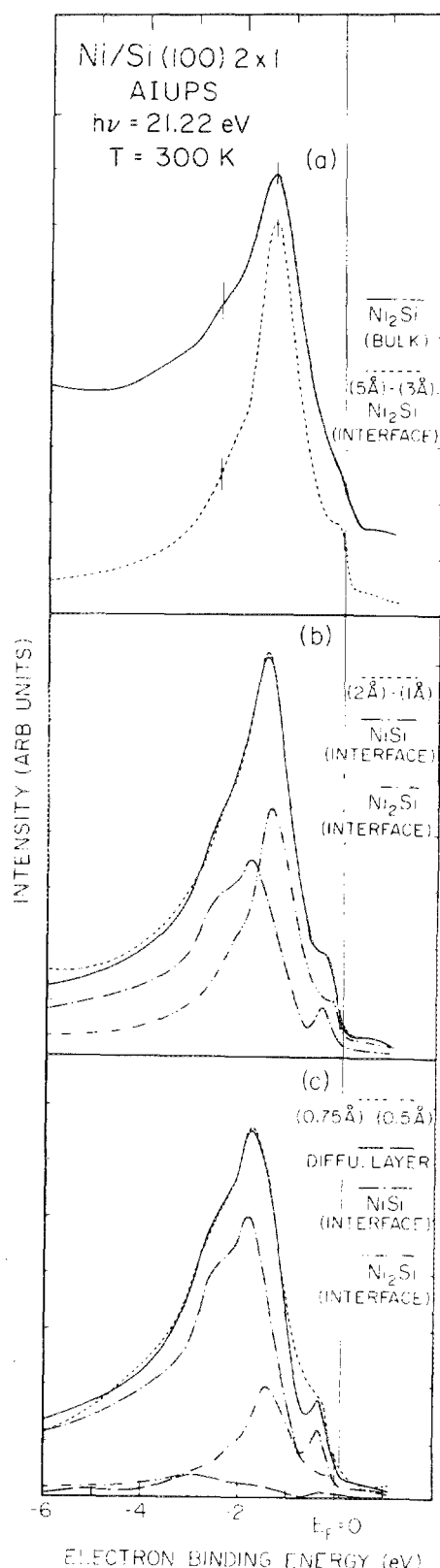


FIG. 4. Lower two panels: Synthesis (solid lines) of experimental difference curves (dotted lines) from diffusion layer spectra, NiSi spectra, and Ni_2Si spectra (see the legend). Upper panel: Difference curve (dotted line) obtained by subtracting 3 \AA spectra from 5 \AA spectra of Fig. 1. Solid line spectra for bulk Ni_2Si .

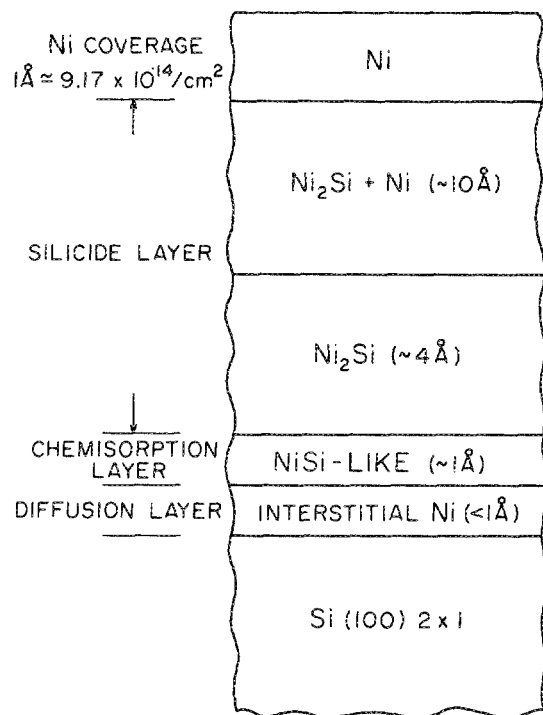


FIG. 5. Schematic representation of a room temperature Ni-Si(100) interface.

Ni atom coverages of about 0.25 \AA , Ni atoms also begin to occupy interstitial sites in the Si lattice forming a diffusion layer. This result is consistent with recent XPS studies²⁰ and channeling results.¹⁵ At Ni atom coverages of about 1.5 \AA the diffusion layer appears to saturate and addition of more Ni atoms permits nucleation of Ni_2Si . The NiSi interface and diffusion layer persist as more Ni atoms are added but in the Ni atom coverage range from $2\text{--}15 \text{ \AA}$, the Ni_2Si phase continues to nucleate and grow. Based on analysis of difference spectra in this range, the Ni_2Si phase appears to have relatively uniform stoichiometry; the work function data shows that this phase becomes nickel rich as the thickness approaches 15 \AA . Ni atoms deposited after 15 \AA of Ni have been deposited begin to form a Ni film. Figure 5 illustrates our best estimate of the structure of a room temperature grown interface.

The procedure we have applied involves obtaining difference curves by subtracting two high resolution EDC's corresponding to different overlayer thicknesses, and then synthesizing this difference curve based on established results for the diffusion layer and bulk phases of NiSi and Ni_2Si . We have repeated this study on Si(111) substrates and have obtained consistent results. The Si(111) surface presents more difficulty due to overlap of the NiSi d -state features at -1.9 eV binding energy with the Si(111) surface state at -1.8 eV binding energy. We have also obtained preliminary results

for Ni-Si(100) interfaces formed at temperatures above 300 K , and this work supports results reported here.

ACKNOWLEDGMENTS

This work was sponsored by the Joint Services Electronics Program (F 4962-77-C-0101) and by NSF (DMR 79-23629).

- ¹P. B. Ghate, Texas Institute Report No. 03-81-44, 1981.
- ²J. L. Freeouf, *Solid State Commun.* **33**, 1059 (1980).
- ³K. N. Tu, *Appl. Phys. Lett.* **27**, 221 (1975).
- ⁴G. Ottaviani, *J. Vac. Sci. Technol.* **16**, 1112 (1979).
- ⁵J. C. Phillips, *Solid State Commun.* **12**, 861 (1973).
- ⁶J. Bardeen, *Phys. Rev.* **71**, 717 (1947).
- ⁷V. Heine, *Phys. Rev. A* **138**, 1689 (1965).
- ⁸J. C. Phillips, *J. Vac. Sci. Technol.* **11**, 947 (1974).
- ⁹J. M. Andrews and J. C. Phillips, *Phys. Rev. Lett.* **35**, 56 (1975).
- ¹⁰G. Ottaviani, K. N. Tu, and J. W. Mayer, *Phys. Rev. Lett.* **44**, 284 (1980).
- ¹¹J. M. Andrews and F. B. Koch, *Solid State Electron.* **14**, 901 (1971).
- ¹²G. Ottaviani, K. N. Tu, W. K. Chu, L. S. Hung, and J. W. Mayer, *J. Appl. Phys.* **53**, 4903 (1982).
- ¹³G. Ottaviani, K. N. Tu, and J. W. Mayer, *Phys. Rev. B* **24**, 3354 (1981).
- ¹⁴K. C. R. Chiu, J. M. Poate, L. C. Feldman, and C. J. Doherty, *Appl. Phys. Lett.* **36**, 544 (1980).
- ¹⁵N. W. Cheung and J. W. Mayer, *Phys. Rev. Lett.* **46**, 671 (1981); N. W. Cheung, R. J. Culbertson, L. C. Feldman, P. J. Silverman, K. W. West, and J. W. Mayer, *ibid.* **45**, 120 (1980).
- ¹⁶H. Ishiura, K. Hikosaka, M. Nagatomo, and S. Furukawa, *Surf. Sci.* **86**, 711 (1979).
- ¹⁷F. d'Heurie, S. Petersson, L. Stolt, and B. Strizker, *J. Appl. Phys.* **53**, 5678 (1982).
- ¹⁸W. K. Chu, H. Krautle, J. W. Mayer, H. Miller, and M. A. Nicolet, *Appl. Phys. Lett.* **25**, 454 (1974).
- ¹⁹P. J. Grunthaner, F. J. Grunthaner, and A. Madhukar, *J. Vac. Sci. Technol.* **20**, 680 (1982).
- ²⁰N. W. Cheung, P. J. Grunthaner, F. J. Grunthaner, J. W. Mayer, and B. M. Ullrich, *J. Vac. Sci. Technol.* **18**, 917 (1981).
- ²¹P. J. Grunthaner, F. J. Grunthaner, and J. W. Mayer, *J. Vac. Sci. Technol.* **17**, 924 (1980).
- ²²P. J. Grunthaner, F. J. Grunthaner, A. Madhukar, and J. W. Mayer, *J. Vac. Sci. Technol.* **19**, 649 (1981).
- ²³P. J. Grunthaner, F. J. Grunthaner, and A. Madhukar, *J. Vac. Sci. Technol.* **21**, 637 (1982).
- ²⁴A. Franciosi, J. H. Weaver, D. G. O'Neill, Y. Chabal, J. E. Rowe, J. M. Poate, O. Bisi, and C. Calandra, *J. Vac. Sci. Technol.* **21**, 624 (1982).
- ²⁵I. Abbati, L. Braicovich, B. DeMichelis, U. del Pennino, and S. Valeri, *Solid State Commun.* **43**, 199 (1982).
- ²⁶I. Abbati, L. Braicovich, U. Del Pennino, B. De Michelis, and S. Valeri, *Le Vide, les Conches Minces* **201**, 959 (1980).
- ²⁷Yu-Jeng Chang and J. L. Erskine, *Phys. Rev. B* **26**, 1 (1982).
- ²⁸Y. J. Chabel, D. R. Hamann, J. E. Rowe, and M. Schluter, *Phys. Rev. B* **25**, 7598 (1982).
- ²⁹A. Franciosi, J. H. Weaver, and F. A. Schmidt, *Phys. Rev. B* **26**, 546 (1982).
- ³⁰K. C. R. Chiu, J. M. Poate, J. E. Rowe, T. T. Sheng, and A. G. Cullis, *Appl. Phys. Lett.* **38**, 988 (1981).
- ³¹L. Wray and M. Pratton, *Thin Solid Films* **15**, 173 (1973).
- ³²D. M. Bylander, L. Kleinman, K. Medrick, and W. R. Grise, *Phys. Rev. B* **26**, 6379 (1982).
- ³³O. Bisi and C. Calandra, *J. Phys. C* **14**, 5479 (1981).
- ³⁴Yu-Jeng Chang and J. L. Erskine, *Phys. Rev. B* **26**, 4766 (1982).
- ³⁵R. M. Walser and R. W. Bene, *Appl. Phys. Lett.* **28**, 624 (1976).
- ³⁶J. L. Erskine, *Phys. Rev. Lett.* **45**, 1446 (1980).
- ³⁷N. Shevchik, *J. Electron Spectros. Relat. Phenom.* **14**, 411 (1978).